Journal of Photochemistry and Photobiology A: Chemistry 205 (2009) 151–155

Contents lists available at ScienceDirect

Journal of Photochemistry and Photobiology A: Chemistry

journal homepage: www.elsevier.com/locate/jphotochem

Fluorescence modulation and photodegradation characteristics of safranin O dye in the presence of ZnS nanoparticles

Maged El-Kemary*, Hany El-Shamy

Chemistry Department, Faculty of Science, Kafrelsheikh University, 33516 Kafr ElSheikh, Egypt

ARTICLE INFO

Article history:
Received 27 November 2008
Received in revised form 30 March 2009
Accepted 27 April 2009
Available online 3 May 2009

Keywords:
Nanoparticles
ZnS
Fluorescence
Dye
Photocatalyst
Degradation

ABSTRACT

ZnS nanoparticles were synthesized using a chemical precipitation method and were characterized with FTIR, transmission electron microscope (TEM), X-ray diffraction analysis (XRD) and UV–vis absorption. XRD analysis shows that the diameter of the particles is 1.6 nm. The interaction between ZnS nanoparticles and safranin O (SO) dye was studied with UV–vis absorption as well as fluorescence emission and excitation spectra. The results show fluorescence enhancement from dye molecules with nanoparticles upon excitation at 325 nm. In contrast, the fluorescence of the dye monitored at 520 nm is quenched by ZnS nanoparticles. ZnS nanoparticles were used as a photocatalyst in order to degrade SO dye. A maximum degradation efficiency of 51% of the dye has been achieved in the presence of ZnS as a nanophotocatalyst at pH 7. Photodegradation of the dye follows second-order kinetics.

1. Introduction

Semiconductor nanoparticles have attracted considerable attention due to their size-dependent photophysical and photochemical properties [1,2]. Such materials are promising for the production of optical sensitizers and photocatalysis [3–5]. Further, they can be used for optoelectronic devices [6,7], electroluminescent applications [8], quantum devices [9], and in novel biomolecular applications, such as DNA detection [10,11]. Zinc sulphide (ZnS) is one of the semiconductor nanomaterials that show promise for the production of optical sensitizers, photocatalysis, electroluminescent materials, optical sensors [12,13] and for solar energy conversion [14]. Some dyes are also used as photosensitizers for solar energy conversion, or as photosensitizers for wide band-gap semiconductors, extending the wavelength absorbed by the system to the visible range [15,16].

Safranin-O (3,7-diamino-2,8-dimethyl-5 phenylphenazinium chloride (SO), Scheme 1) is a phenazine dye, that has been used as a photosensitizer in electron- and energy-transfer reactions [17]. Also, it is used as a sensitizer in visible light photopolymerization [18]. Phenazine dyes are used in the textile industry and are photodegraded under UV light using a semiconductor as a catalyst [19]. We have examined the fluorescence quenching of safranin T by thiones in micelles and homogeneous media [20]. Youqiu et al. reported the decrease in the absorbance and fluorescence quenching for safranine T by gold nanoparticles [21]. Recently, Hamity et al. have investigated the effect of CdS nanoparticles on the photodegradation of SO [22].

In the present work, we describe the synthesis and characterization of ZnS nanoparticles. Also, we report the interaction between ZnS nanoparticles and SO dye and the possible roles of the nanoparticles as a catalyst for photodegradation of the dye.

2. Experimental

2.1. Materials

Safranin O (Sigma), zinc acetate (Aldrich), thiourea (Aldrich) and ammonia (Aldrich) were of analytical grade and were used without further purification. Deionized water was used to prepare the buffer solution.

2.2. Equipment

The morphology of ZnS nanoparticles was observed by a transmission electron microscope (TEM, JEM-200CX). UV–vis absorption spectra were measured on a Shimadzu UV-2450 spectrophotometer. Fluorescence spectra were recorded on a Shimadzu RF-5301PC spectrofluorometer. The FT-IR analysis was made on a JASCO spectrometer 4100. The powder X-ray diffraction (XRD) analysis was made on a Rigaku 2550D/max VB/PC X-ray diffractometer using CuKα radiation (λ = 1.54056 Å).

* Corresponding author. Tel.: +20 100 297 421; fax: +20 473 223 415.
E-mail address: elkemary@yahoo.com (M. El-Kemary).

1010-6030/$ – see front matter © 2009 Published by Elsevier B.V.
doi:10.1016/j.jphotochem.2009.04.021

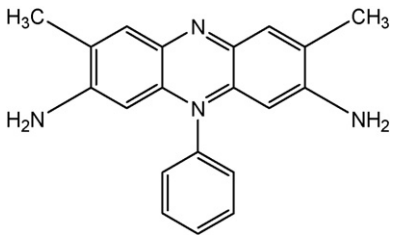

Scheme 1. The molecular structure of safranine O.

2.3. Synthesis of ZnS nanoparticles

ZnS nanoparticles were synthesized by a chemical precipitation method using ammonia as a capping agent for surface passivation. A solution of thiourea (0.5 M) was added drop wise to an aqueous solution of zinc acetate (0.5 M). An ammonia solution was added slowly to the mixture to form the complex and to maintain the pH between 9 and 10. The solution was stirred for 15 min. The precipitated particles were filtered using Whatman 40 filter paper. To remove the last traces of adhered impurities, the particles were washed several times using deionized water. The washed particles were dried in a desiccator.

2.4. Photodegradation experiments

Photodegradation experiments were performed with a solution of 50% (molar) ZnS nanoparticles and 50% (molar) SO dye. The pH of both solutions was adjusted to 7. Aliquots of the sample were withdrawn and placed into a quartz cuvette. The cuvette was placed in front of a Xenon Lamp where the solution was exposed to ultraviolet light (UV) for variable time intervals and then the sample was quickly subjected to emission measurement.

3. Results and discussions

3.1. Structure and characterization

Fig. 1(a) shows a typical TEM image of ZnS nanoparticles. It can be seen that ZnS nanoparticles are polydispersed and almost spherically shaped. The XRD spectra of ZnS are shown in Fig. 1(b). We observe three reflection peaks at 2θ values of 28·978°, 48·519°, and 57·927° corresponding to the (1 1 1), (2 2 0), and (3 1 1) diffraction planes, respectively, of the cubic crystalline structure of ZnS. These values are close to those reported by Pant et al. [23]. The mean particle diameter d (1.6 nm) was estimated using the most intense peak of the (1 1 1) plane of ZnS, from the Debye–Scherrer formula (Eq. (1)) [24].

$$d(\text{Å}) = \frac{k\lambda}{\beta \cos\theta} \quad (1)$$

where k is an empirical constant equal to 0.9, λ is the wavelength of the X-ray source (1.5405 Å), β is the full width at half maximum of the diffraction peak, and θ is the angular position of the peak.

Fig. 2 shows the FTIR analysis of ZnS nanoparticles. The broad band at 3401 cm^{-1} is attributed to water of hydration present in the solution. The weak peaks located at 2870 cm^{-1} and 2939 cm^{-1} are assigned to symmetric and asymmetric C–H stretches. C–H bonds are present in monoacetate groups as intermediate products [25]. The peaks at 1554 cm^{-1} and 1407 cm^{-1} are attributed to asymmetric and symmetric stretching vibrations of the carboxylate ions ($-COO^-$) [26]. The appearance of these vibrations is due to the presence of monoacetate. The peak at 3401 cm^{-1} can be attributed to N–H stretching vibration of the $-NH_2$ group on the surface of the ammonia capped ZnS nanoparticles. The peaks appearing at

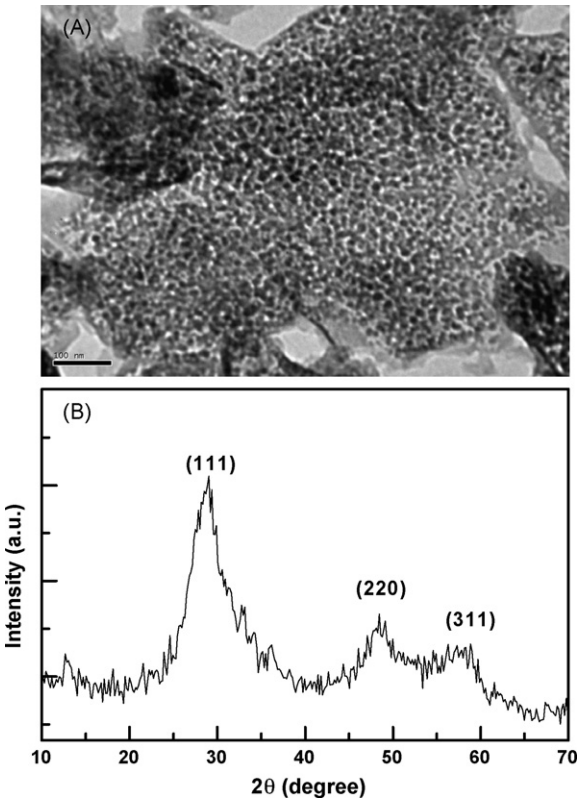

Fig. 1. TEM image (a) and XRD (b) spectra of ZnS nanoparticles.

483 cm^{-1} and 680 cm^{-1} are assigned to the Zn–S stretching vibration.

Fig. 3 shows the UV–vis absorption spectra of ZnS nanoparticles in the absence and presence of SO dye. ZnS nanoparticles show an intense absorption peak at 236 nm corresponding to a band gap of 5.27 eV. The band gap of the nanoparticles is calculated from the following equation:

$$E = \frac{hc}{\lambda} \quad (2)$$

where E is the band-gap energy, h is Planck's constant, c is the speed of light, and λ is the wavelength of the absorption edge in absorption spectrum. The calculated band gap (5.27 eV) for ZnS nanoparticles

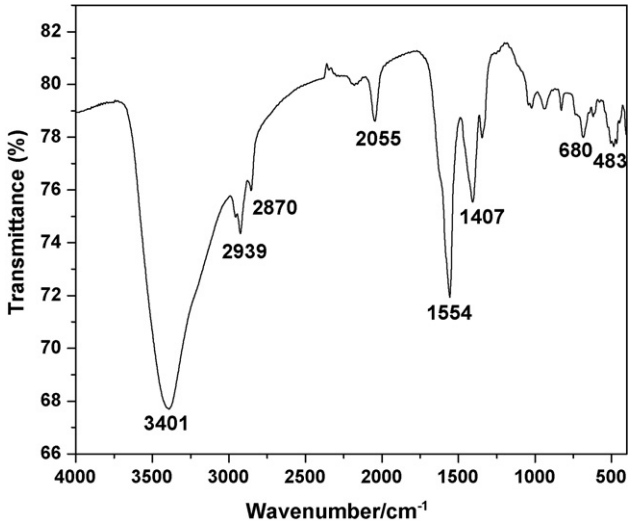

Fig. 2. FT-IR spectra of ZnS nanoparticles.

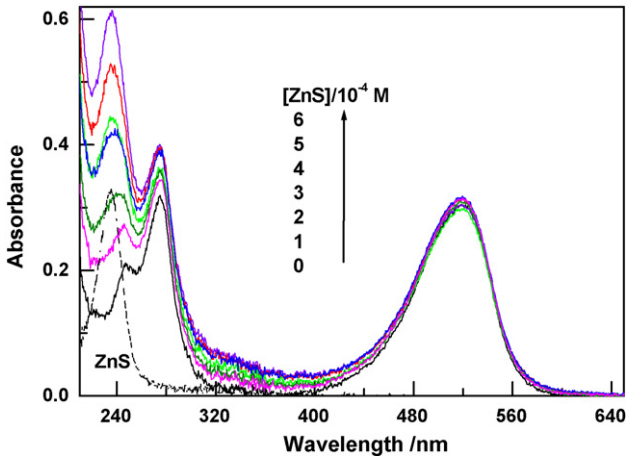

Fig. 3. UV–vis absorption spectra of ZnS nanoparticles (dotted line) and SO dye in the absence and presence of ZnS nanoparticles (solid lines).

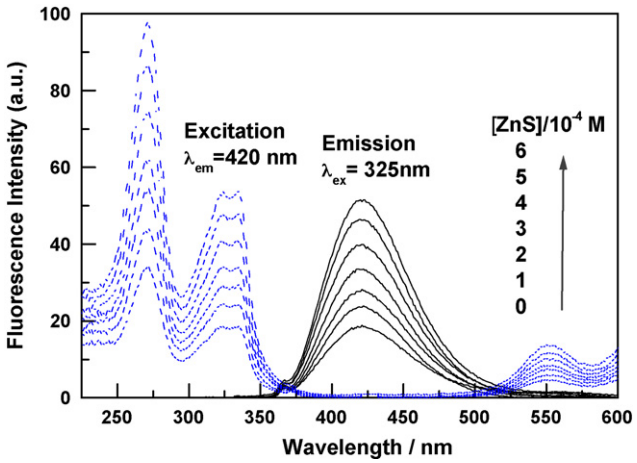

Fig. 4. Emission spectra (solid lines, λ_{ex} = 325 nm) and corresponding excitation spectra (dotted lines, λ_{em} = 420 nm) from pure dye and dye with variable concentration of ZnS nanoparticles.

is blue-shifted from that of bulk ZnS (3.66 eV), which suggests the influence of quantum confinement.

The absorption band observed around 236 nm, indicates a relatively narrow size distribution of ZnS nanoparticles. From the position of absorption edge, the average particle size can be determined using Henglein's empirical relation between particles size and absorption onset (λ) [27,28] according to the following equation:

$$2R = \frac{0.1}{(0.138 - 0.0002345\lambda)\,\text{nm}} \quad (3)$$

where (2*R*) is the average diameter of the particles. From Fig. 3, the absorption maximum (λ) is 236 nm and from Eq. (2) the particle size is estimated to be 1.2 nm, which is slightly smaller than that measured using XRD.

3.2. Interaction of nanoparticles with SO dye

The SO dye molecules exhibit two absorption peaks at 274 nm and 520 nm, in addition to one weak broad peak at 325 nm and one shoulder at 246 nm, Fig. 3. It can be noted that addition of ZnS nanoparticles to SO dye leads to enhancement of the absorption intensity at 246 nm, 274 nm, and 325 nm without significant effect on the absorption intensity at 520 nm. The absorption enhancement at 246 nm is more significant and accompanied with a blue shift. The results suggest an interaction between the nanoparticles and SO. The absorption spectra of samples of dye molecules with higher concentrations of ZnS nanoparticles (5-6 × 10^{-4} M^{-1}) are the sum of the spectra recorded for the dye and the ZnS nanoparticles measured separately. Similar results were observed by Franzen et al. while studying the optical properties of rhodamine 6G dye molecules with silver nanoparticles [29].

To support the hypothesis of the interaction between the SO dye and nanoparticles, we measured the luminescence spectra from solutions of the pure dye and solutions of the dye molecules with variable concentrations of ZnS nanoparticles at an excitation wavelength of 325 nm, Fig. 4. It is readily seen that the emission spectra of SO exhibits an emission peak at 420 nm, which shows an enhancement of intensity in the presence of ZnS nanoparticles. The corresponding fluorescence excitation spectra of SO monitored at 420 nm consists of two distinct peaks at 270 nm and ~325 nm, Fig. 4. Their intensity gradually increases with increasing concentration of ZnS nanoparticles, Fig. 4. These results support the concept of the interaction between ZnS nanoparticles and SO dye.

The observed fluorescence excitation spectra (Fig. 4) show two important features. First, they are considerably different from the absorption spectra (Fig. 3) suggesting that the excited states are subject to electronic changes upon binding to the nanoparticles. Second, they demonstrate the absence of mirror image behavior of the fluorescence spectra, due to changes of the molecular orbital symmetries of the dye in the presence of ZnS nanoparticles. The observed enhancement of the excitation and emission rate of the dye is probably due to the existence of a localized electromagnetic field near the nanoparticle when a fluorophore is placed in the close vicinity of the nanoparticle. Similar enhancement in emission spectra from dye molecules with nanoparticles was observed by Haes et al. [30].

In contrast to a fluorescence enhancement of SO in the presence of ZnS nanoparticles upon excitation at 325 nm, the fluorescence monitored at 520 nm is quenched by ZnS nanoparticles, Fig. 5. The second-order quenching constant K_{sv} was determined from the Stern–Volmer (SV) plots using linear regression according to the relation.

$$\frac{I_0}{I} = 1 + K_{sv}[Q] \quad (4)$$

where I_0 and I are the relative fluorescence intensities in the absence and presence of quencher of concentration [Q]. Typical SV plots are linear in the investigated concentration range as shown in the inset of Fig. 5, suggesting that only one type of quenching

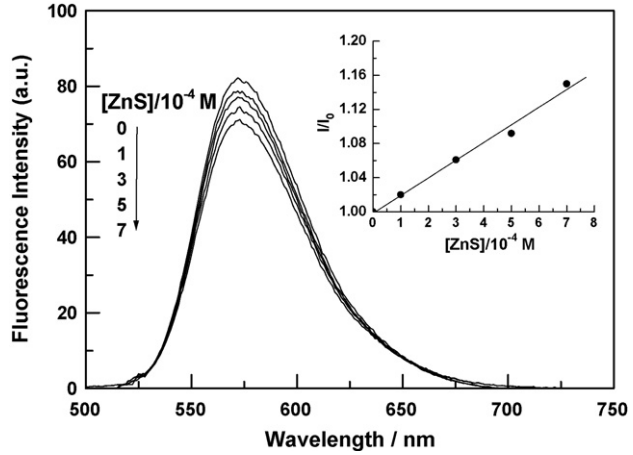

Fig. 5. Fluorescence quenching of SO dye by ZnS nanoparticles at pH 7, λ_{ex} = 520 nm. The inset shows the Stern–Volmer plot.

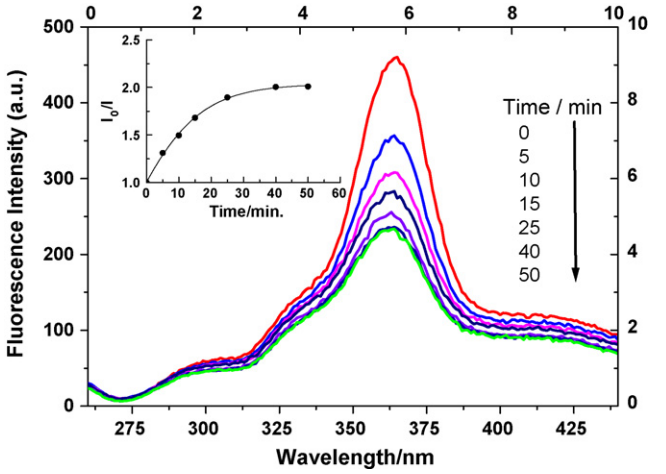

Fig. 6. Quenching effects of SO dye (1.0×10^{-5} M) with ZnS fluorescence (λ_{ex} = 236 nm) exposed to UV light. Inset shows a plot of fluorescence intensity as a function of photodegradation time.

occurs. The regression equation is represented by:

$$\frac{I_0}{I} = 1.01 + 207[\mathrm{SO}] \quad (5)$$

The correlation coefficient is 0.995 and the standard deviation is 0.007.

Internal energy transfer requires good overlap between the emission spectrum of the donor and the absorption spectrum of the acceptor. Because of the large Stokes shift, the overlap of the absorption and emission spectra obtained is not large enough to support the energy-transfer process. Enhancement and quenching of luminescence has been explained in terms of electron transfer from fluorophore to the nanoparticles [31]. When the nanoparticles are in close proximity to the fluorophore, quenching of the luminescence occurs, whereas when nanoparticles are located at longer and system-dependent distances, enhancement in luminescence may be observed [32]. These effects have been explained by coupling of surface plasmon resonances from the nanoparticles and the attached fluorophore.

It is possible with these very small ZnS nanoparticles that mid-band-gap surface trap states could serve to quench the SO dye fluorescence. These types of states will not be observed in the ZnS UV–vis absorption spectra but may provide the proper energy match with the SO excited state to serve as a trap site for the excited SO electron.

3.3. Photocatalytic degradation of SO dye

To test for the photodegradation of SO dye by ZnS nanoparticles, a solution containing SO dye and ZnS nanoparticles is photoirradiated by UV light. At periodic intervals of time, aliquots of the sample were withdrawn and the emission spectra were recorded. Fig. 6 shows the quenching efficiency of SO dye (1.0×10^{-5} M) in the presence of ZnS as a function of time. Clearly, the fluorescence intensity at 365 nm decreases with a slight blue shift as a function of photodegradation time. The photodegradation efficiencies increase with time, reaching a plateau. At which point the degradation efficiency (inset of Fig. 6) was calculated using:

$$\%D = 100 \times \left[\frac{C_0 - C}{C_0}\right] \quad (6)$$

where C_0 and C are the concentrations of dye before and after irradiation. The maximum degradation efficiency is about 51%, occurring after about 40 min. For ZnS nanoparticles doped with manganese, nickel, and copper, the degradation efficiency of SO dye increased to 85–93% [33], possibly due to an increase of the applicable surface of the photocatalyst or accelerated migration of holes to the surface of the nanoparticles. It is important to note that photoirradiation of the SO dye in the absence of ZnS nanoparticles resulted in no significant change in the emission spectra.

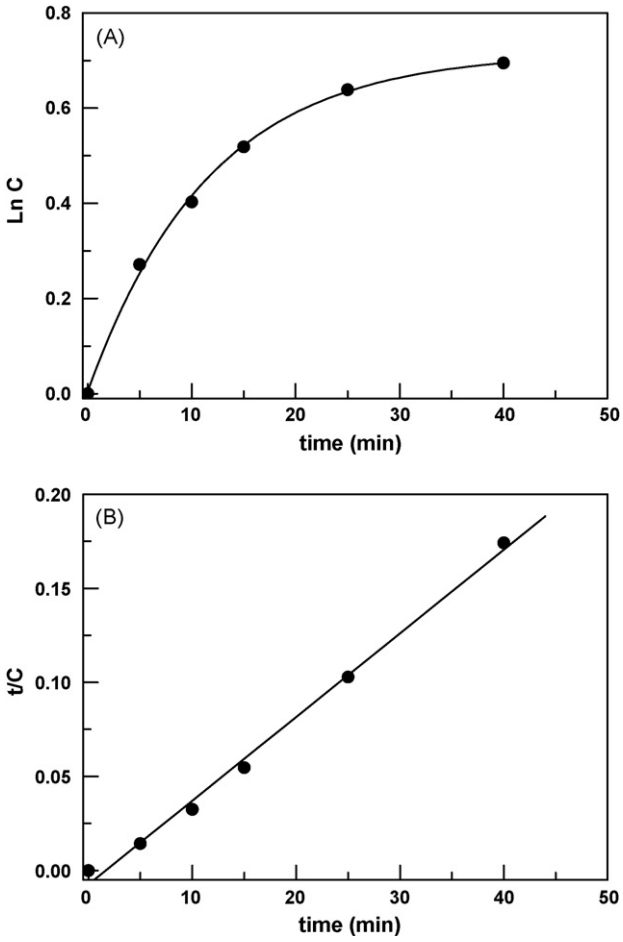

Fig. 7. First-order (A) and second-order (B) plot for the kinetic photodegradation of SO in the presence of ZnS nanoparticles.

In order to check the kinetics for the photolysis of SO in the presence of ZnS, a plot of ln C versus time is performed, Fig. 7A. A downward concave curvature is observed, indicating that first-order kinetics are ruled out.

A linear relationship is observed between t/C_t and irradiation time, Fig. 7B, following the pseudo-second-order-kinetic rate expression [34]:

$$\frac{t}{C_t} = \frac{1}{k_{\mathrm{app}} C_0^2} + \frac{1}{C_0} \quad (7)$$

The linear plot of t/C_t versus time indicates that the reaction follows pseudo-second-order kinetics. The apparent rate constant k_{app} is obtained from the intercept. The observed value of the corresponding rate constant is 4.3×10^{-3} min^{-1}. A possible explanation for second-order photodegradation kinetics is the aggregation or dimer formation with increasing dye concentration. Similar behavior has been reported recently for SO with CdS nanoparticles [22]. Many dyes show this characteristic behavior [35].

Photodegradation of a dye is initiated by photoexcitation of the semiconductor. Light-induced electron/hole pair formation in semiconductor particles, accompanied by subsequent interfacial electron (hole) transfer, has always been considered as the first step

of the photocatalytic action of semiconductor nanoparticles [36,37]. The high oxidative potential of holes can lead to direct and indirect oxidation of dyes. In the indirect oxidation process of dyes, hydroxide radicals ($OH^{\bullet}$) are formed from combination of holes with water molecules and/or hydroxide anions (Eqs. (9) and (10)). Primary photoproducts resulting from interfacial electron–hole transfer, i.e. radical ions undergo further transformations leading to the formation of final photoproducts, Eq. (11) [5]. The proposed mechanism for dye degradation using photocatalysts (P) was suggested as follows [5]:

$$P + h\nu \rightarrow h^{+}VB + e^{-}CB \quad (8)$$

$$OH^{-} + h^{+}VB \rightarrow OH^{\bullet} \quad (9)$$

$$H_2O + h^{+}VB \rightarrow OH^{\bullet} + H^{+} \quad (10)$$

$$\text{Dye} + h^{+}VB \rightarrow \text{Dye}^{\bullet+} \rightarrow \text{Final species} \quad (11)$$

4. Conclusion

ZnS nanoparticles with extremely small size (1.6 nm) were synthesized via a chemical precipitation method. It is found that luminescence properties of dye molecules are modulated by adding small quantities of colloidal ZnS nanoparticles. Coupling of dye molecules with ZnS nanoparticles leads to many interesting optical and electronic properties which may be relevant for a variety of applications such as biological sensing, light emitting diodes, etc. The photodegradation of the dye molecules in the presence of ZnS nanoparticles follows second-order kinetics with a degradation efficiency of ~51%.

Acknowledgements

A Kafrelsheikh University grant is gratefully acknowledged. We thank Professor S. Buckner, Saint Louis University, for his useful discussions.

References

[1] H. Weller, U. Koch, M. Gutièrrez, A. Henglein, Photochemistry of colloidal metal sulfides, Ber. Bunsenges. Phys. Chem. 88 (1984) 649–656.
[2] J.P. Kuczynski, B.H. Milosavijevic, J.K. Thomas, Effect of the synthetic preparation on the photochemical behavior of colloidal CdS, J. Phys. Chem. 87 (1983) 3368–3370.
[3] M. Kanemoto, T. Shiragami, C. Pac, S. Yanagida, Semiconductor photocatalysis. Effective photoreduction of carbon dioxide catalyzed by ZnS quantum crystallites with low density of surface defects, J. Phys. Chem. 96 (1992) 3521.
[4] A.L. Linsebigler, G.Q. Lu, J.T. Yates, Photocatalysis on TiO_2 surfaces: principles, mechanisms, and selected results, Chem. Rev. 95 (1995) 735.
[5] M.R. Hoffmann, S.T. Martin, W.Y. Choi, D.W. Bahnemann, Environmental applications of semiconductor photocatalysis, Chem. Rev. 95 (1995) 69.
[6] M. Kastner, Artificial atoms, Phys. Today 46 (1993) 24.
[7] L.E. Brus, Quantum crystallites and nonlinear optics, Appl. Phys. A 53 (1991) 465.
[8] V. Colvin, M. Schlamp, A.P. Alivisatos, Light-emitting-diodes made from cadmium selenide nanocrystals and a semiconducting polymer, Nature 370 (1994) 354.
[9] E. Corcoran, Trends materials: diminshing dimensions, Sci. Am. 263 (1990) 74.
[10] A.P. Alivisatos, K.P. Johnsson, X. Peng, T.E. Wilson, C.P. Loweth, M.P. Bruchez Jr., P.G. Schultz, Organization of nanocrystal molecules using DNA, Nature 382 (1996) 609.
[11] Y. Li, J. Chen, C. Zhu, L. Wang, D. Zhao, S. Zhuo, Y. Wu, Preparation and application of cysteine-capped ZnS nanoparticles as fluorescence probe in the determination of nucleic acids, Spectrochim. Acta A 60 (2004) 1719–1724.
[12] O.S. Wolfbeis, Materials for fluorescence-based optical chemical sensors, J. Mater. Chem. 15 (2005) 2657–2669.
[13] K.E. Sapsford, T. Pons, I.L. Medintz, H. Mattoussi, Biosensing with luminescent semiconductor quantum dots, Sensors 6 (2006) 925–953.
[14] A.A. Nada, H.A. Hamed, M.H. Barakat, N.R. Mohamed, T.N. Veziroglu, Enhancement of photocatalytic hydrogen production rate using photosensitized TiO_2/RuO_2–MV^{2+}, Int. J. Hydrogen Energy 33 (2008) 3264–3269.
[15] D. Chatterjee, A. Mahata, Visible light induced photodegradation of organic pollutants on dye adsorbed TiO_2 surface, J. Photochem. Photobiol. A: Chem. 153 (2002) 199–204.
[16] L.M. Peter, Characterization and modelling of dye-sensitized solar cells, J. Phys. Chem. C 111 (2007) 6601–6612.
[17] S. Saravanan, P. Ramamurthy, Excited singlet state reaction of phenosafranine with electron donors role of the heavy-atom effect in triplet induction, J. Chem. Soc., Faraday Trans. 94 (1998) 1675–1679.
[18] M.V. Encinas, A.M. Rufs, M.G. Neumann, C.M. Previtali, Photoinitiated vinyl polymerization by safranine T/triethanolamine in aqueous solution, Polymer 37 (1996) 1395–1398.
[19] V.K. Gupta, R. Jain, A. Mittal, M. Mathur, S. Sikarwar, Photochemical degradation of the hazardous dye Safranin-T using TiO_2 catalyst, J. Colloid Interface Sci. 309 (2007) 464–469.
[20] M. El-Kemary, R. Khedr, S.H. Etaiw, Fluorescence decay of singlet excited-state of safranine T and its interaction with ground-state of pyridinthiones in micelles and homogeneous media, Spectrochim. Acta A 58 (2002) 3011–3019.
[21] H. Youqiu, L. Shaopu, L. Qin, L. Zhongfang, H. Xiaoli, Absorption, fluorescence and resonance Rayleigh scattering spectral characteristics of interaction of gold nanoparticle with safranine T, Sci. China Ser. B: Chem. 48 (2005) 216–226.
[22] M. Hamity, R.H. Lema, C.A. Suchetti, H.E. Gsponer, UV–vis photodegradation of dyes in the presence of colloidal Q-CdS, J. Photochem. Photobiol. A: Chem. 200 (2008) 445–450.
[23] H.C. Pant, M.K. Patra, S.C. Negi, A. Bhatia, S.R. Vadera, N. Kumar, Studies on conductivity and dielectric properties of polyaniline–zinc sulphide composites, Bull. Mater. Sci. 29 (2006) 379–384.
[24] B.D. Cullity, Elements of X-ray Diffraction, A.W.R.C. Inc., Massachusetts, 1967.
[25] R.C. Perez, O.J. Sandoval, J.M. Mann, A.M. Galvan, G.T. Delgado, Influence of annealing temperature on the formation and characteristics of sol-gel prepared ZnO films, J. Vac. Sci. Technol. A 17 (1999) 1811–1816.
[26] J. Zhao, L. Zhao, X. Wang, Preparation and characterization of ZnO/ZnS hybrid photocatalysts via microwave-hydrothermal method, Environ. Sci. Eng. China 2 (2008) 415–420.
[27] M. Moffitt, E. Aisenberg, Size control of nanoparticles in semiconductor-polymer composites. 1. Control via multiplet aggregation numbers in styrene-based random ionomers, Chem. Mater. 7 (1995) 1178–1184.
[28] R. He, X.-F. Qian, J. Yin, H. Xi, L. Bian, Z.-K. Zhu, Formation of monodispersed PVP-capped ZnS and CdS nanocrystals under microwave irradiation, Colloids Surf. A 220 (2003) 151–157.
[29] S. Franzen, J.C. Folmer, W.R. Glomm, R. O'Neal, Optical properties of dye molecules adsorbed on single gold and silver nanoparticles, J. Phys. Chem. A 106 (2002) 6533–6540.
[30] A.J. Haes, C.L. Haynes, A.D. McFarland, S. Zou, G.C. Schatz, R.P. Van Duyne, Plasmonic materials for surface-enhanced sensing and spectroscopy, Mater. Res. Soc. Bull. 30 (2005) 368–375.
[31] J.R. Lakowicz, C.D. Geddes, I. Gryczynski, J. Malicka, Z. Gryczynski, K. Aslan, J. Lukomska, E. Matveeva, J. Zhang, R. Badugu, J. Huang, Advances in surface-enhanced fluorescence, J. Fluoresc. 14 (2004) 425–441.
[32] J. Zhang, J.R. Lacowicz, A model for DNA detection by metal-enhanced fluorescence from immobilized silver nanoparticles on solid substrate, J. Phys. Chem. B110 (2006) 2387–2392.
[33] H. Pouretedal, A. Norozi, M. Keshavarz, A. Semnani, Nanoparticles of zinc sulphide doped with manganese, nickel and copper as nanophotocatalyst in the degradation of organic dyes, J. Hazard. Mater. 162 (2009) 674–681.
[34] Z. Zainal, C.Y. Lee, M.Z. Hussein, A. Kassim, N.A. Yusof, Electrochemical-assisted photodegradation of mixed dye and textile effluents using TiO_2 thin films, J. Hazard. Mater. 146 (2007) 73–80.
[35] A. Niazi, A. Yazdanipour, J. Ghasemi, M. Kubista, Spectrophotometric and thermodynamic study on the dimerization equilibrium of ionic dyes in water by chemometrics method, Spectrochim. Acta A 65 (2006) 73–78.
[36] Y. Wang, Photophysical and photochemical processes of semiconductor nanoclusters, in: D. Neckers (Ed.), Advances in Photochemistry, vol. 19, 1995, p. 179.
[37] B. Ohtani, S. Kusakabe, K. Okada, S. Tsuru, K. Izawa, Y. Amino, S. Nishimoto, Stereoselective synthesis of piperidine-2,6-dicarboxylic acids by photocatalytic reaction of aqueous cadmium(II) sulfide dispersion, Tetrahedron Lett. 36 (1995) 3189–3191.